Electrical and Thermal Transport through Silver Nanowires and Their Contacts – Effects of Elastic Stiffening

Yang Zhao,[1] Matthew L. Fitzgerald,[1] Yi Tao,[1,2] Zhiliang Pan,[1] Godfrey Sauti,[3] Dongyan Xu,[4] Ya-Qiong Xu,[5,6] and Deyu Li[1,*]

[1]*Department of Mechanical Engineering, Vanderbilt University, Nashville, TN, 37235, USA*
[2]*School of Mechanical Engineering and Jiangsu Key Laboratory for Design and Manufacture of Micro-Nano Biomedical Instruments, Southeast University, Nanjing 210096, China*
[3]*NASA Langley Research Center, Hampton, VA 23681-2199*
[4]*Department of Mechanical and Automation Engineering, The Chinese University of Hong Kong, Shatin, New Territories, Hong Kong Special Administrative Region, China*
[5]*Department of Electrical Engineering and Computer Science, Vanderbilt University, Nashville, TN, 37235, USA*
[6]*Department of Physics and Astronomy, Vanderbilt University, Nashville, TN, 37235, USA*

*: Author to whom correspondence should be addressed
E-mail: deyu.li@vanderbilt.edu

Abstract

Silver nanowires have been widely adopted as nanofillers in composite materials used for various applications. Electrical and thermal properties of these composites are critical for proper device operation, and highly depend on transport through the nanowires and their contacts, yet studies on silver nanowires have been limited to one or two samples and no solid data have been reported for individual contacts. Through systematic measurements of silver nanowires of different sizes, we show that the Lorenz number increases with decreasing wire diameter and has a higher value at wire contacts. Examination of the corresponding electrical and thermal conductivities indicates that these changes are due to contributions of phonons that become more important as a result of elastic stiffening. The derived contact thermal conductance per unit area between silver nanowires is ~10 times that between carbon nanotubes. This helps to explain the more significant thermal conductivity enhancement of silver nanowires-based composites.

Keywords: elastic stiffening, Lorenz number, electron-phonon interaction, silver nanowire, contact resistance

Silver nanowires, owing to their excellent electrical, thermal and optoelectronic properties, are finding more and more applications as essential components in flexible electronic devices, optoelectronic energy converters, and thermal interface materials.[1–4] So far, there have been several reports on the transport properties of silver nanowires.[5–9] However, the reported studies are often based on limited samples and the results are not consistent with each other; and therefore, it is important to conduct systematic studies to obtain consistent trends of transport properties as a function of the nanowire size. In addition, as nanofillers, electrical and thermal contact resistance between silver nanowires are critical for the overall properties of the resulting composites; however, no direct experimental data have been reported on the resistance at these nanoscale contacts.

One interesting observation for silver nanowires is that elastic stiffening occurs as the wire diameter drops below ~100 nm.[10–12] Recently, it has been shown that for silicon nanowires of < 30 nm diameters, elastic/acoustic softening is responsible for the observed thermal conductivity reduction beyond what the classical size effect predicts.[13,14] It follows to ask whether and how elastic stiffening alters electrical and thermal transport in thin silver nanowires.

In this letter, we report on systematic measurements of electrical and thermal transport properties of silver nanowires with diameters ranging from 38 to 84 nm, which allows for examination of the elastic stiffening effects on the transport properties. Importantly, we also extract previously unavailable data on the contact resistance between individual silver nanowires. These results provide important insights into the transport properties of silver nanowire-based nanocomposites.

Fig. 1a shows a scanning electron microscopy (SEM) image of a silver nanowire with a pentagonal cross-section. For wires with non-circular cross-sections, we use the hydraulic diameter

($D_h = 4A/P$, where A is cross-sectional area and P is perimeter) to represent the wire characteristic size.[15,16] To reduce the contact resistance, we conducted electron beam induced deposition (EBID) of Pt at the wire-membrane contacts and Fig. 1b plots the extracted thermal conductance *versus* temperature after the first and second round of EBID. The overlapping values indicate that the contact thermal resistance becomes negligible as compared to the resistance of the nanowire[17] (see Supporting Information).

Fig. 2a shows the thermal conductivity of a silver nanowire with $D_h = 84$ nm and $L_s = 44$ μm, which demonstrates an increasing trend with temperature. The room-temperature (300 K) thermal conductivity is 332 W/m-K, ~22.6% lower than the bulk value of 429 W/m-K.[18] However, compared to the reported experimental data,[5,6,9] which range from 200 to 300 W/m-K for silver wires of 90-230 nm in diameter and 7-28 μm long, our results represent a higher thermal conductivity for a smaller wire. For silver nanowires of larger diameters and shorter lengths, we found that the contact thermal resistance between the wire and suspended membranes might not be negligible (see Fig. S1), which could lead to a lower effective thermal conductivity. Another factor that could contribute to the lower thermal conductivity in the literature is the overestimation of the wire diameter with an assumption of a circular cross-section. In our case, the pentagonal cross-section corresponding to $D_h = 84$ nm actually shows an outer-diameter of 96 nm as measured directly from the top-view SEM micrograph.

The temperature dependence of the electrical resistivity of the same wire is plotted in Fig. 2b. Compared to the bulk value of 1.63×10^{-8} Ω-m,[19] the room-temperature electrical resistivity (2.13×10^{-8} Ω-m) of the wire is 30.7% higher. If we directly fit the data using the widely adopted Bloch-Grüneisen (BG) formula[20]

$$\rho(T) = \rho_0 + \rho_{e-ph}(T), \quad (1)$$

$$\rho_{e-ph}(T) = \alpha_{e-ph}\left(\frac{T}{\Theta_D}\right)^5 \int_0^{\frac{\Theta_D}{T}} \frac{x^5}{(e^x-1)(1-e^x)}dx, \quad (2)$$

where ρ_0 is the residual resistivity due to defect scattering, $\rho_{e\text{-}ph}$ is the resistivity arising from electron-phonon (e-ph) interactions, $\alpha_{e\text{-}ph}$ is a constant characterizing e-ph coupling, and Θ_D is the Debye temperature, the best fitting (see Fig. S5) for the 84 nm diameter wire gives a Debye temperature of 128 K, much smaller than the bulk value of 230 K.[21] In addition, $\rho_0 = 1.67\times10^{-9}$ Ω-m, which is two orders of magnitude higher than the bulk value. Considering the actually enhanced Young's modulus in silver nanowires, the resulting lower Θ_D cannot be justified. More importantly, we found that the fitting gets worse for smaller nanowires, which clearly indicates that a better model is needed.

The BG model does not explicitly consider electron scattering at the nanowire surface, which leads to much larger residue resistivity; at low temperatures, temperature-dependent small angle e-ph scattering of electrons renders the resistance from boundary scattering at the nanowire surface changes with temperature, leading to a much lower Θ_D if its effect is absorbed into the BG fitting.[5] To explicitly reflect the surface contribution, we calculate a reduction function following the Fuchs-Sondheimer approach, which relates the nanowire resistivity with the bulk value as[22,23]

$$\left(\frac{\rho_{bulk}}{\rho_{nw}}\right)_{p=0,l} = \frac{3}{2\pi r_0^2}\int_0^{r_0=\frac{D_h}{2}} rdr \int_0^{2\pi} d\varphi \int_0^{\pi} sin\theta cos^2\theta \left(1 - e^{-\frac{\sqrt{r^2cos^2\varphi + r_0^2 - r^2} - rcos\varphi}{lsin\theta}}\right) d\theta, \quad (3)$$

$$\left(\frac{\rho_{bulk}}{\rho_{nw}}\right)_{p,l} = (1-p)^2 \sum_{m=1}^{\infty}\left\{mp^{m-1}\left(\frac{\rho_{bulk}}{\rho_{nw}}\right)_{p=0,\frac{l}{m}}\right\}, \quad (4)$$

where ρ_{bulk} is the electrical resistivity of bulk silver that can be modeled using Eq. (1) and (2), ρ_{nw} is the electrical resistivity of the nanowire, r is the radius, θ is the polar angle between the electron

traveling direction and the wire axial direction, φ is the azimuthal angle, l is the electron mean free path (EMFP) in bulk silver, and p is the specularity parameter at nanowire surface. For simplicity, the above derivation is based on a circular cross section. Importantly, it has been shown that as long as the surface area to volume ratio (or hydraulic diameter) is the same, the surface scattering effect is approximately the same.[14] In this approach, with Θ_D = 230 K, the fitting curve matches the measured data almost perfectly with the following parameters: ρ_0 = 8.15×10^{-11} Ω-m, $\alpha_{e\text{-}ph}$ = 5.782×10^{-8} Ω-m, and p = 0.65, which provide minimum variance.

Fig. 2c depicts the electrical and thermal EMFP of the nanowire. The electrical EMFP ($l_{e,nw}$) is calculated as $l_{e,nw} = \frac{\sigma m v_F}{ne^2}$, where n is the free electron density, m the electron mass, and v_F the Fermi velocity.[24] First principles calculations have suggested that at room temperature phonons in bulk silver only contribute ~1.07% to the total thermal conductivity.[25] Because phonon MFP is very small in silver (1-10 nm),[25] the lattice thermal conductivity of the 84 nm diameter wire can be regarded approximately the same as that of the bulk ($\kappa_{ph,bulk}$ = ~4.6 W/m-K), which is ~1.4% of the measured nanowire thermal conductivity, still a small percentage compared to the electron contribution. As the electronic thermal conductivity is approximately equal to the total thermal conductivity, the thermal EMFP ($l_{th,nw}$) is calculated as $l_{th,nw} = \frac{3\kappa}{C_e v_F}$, where $C_e = \frac{\pi^2 n k_B^2 T}{2E_F}$ is the heat capacity per unit volume in which E_F is the Fermi energy.[5,20] For silver, n is 5.85×10^{28} m^{-3}, E_F is 5.48 eV and v_F is 1.39×10^6 m/s.[24] The calculated electrical and thermal EMFPs both decrease as the temperature increases due to enhanced e-ph scattering at higher temperatures. At higher temperatures, e-ph interactions mainly occur through large angle scattering, which poses resistance to both electrical and thermal transport.[21] However, as temperature drops, the dominant phonon wave vector decreases, which allows for more electron scattering through small angles that has a

marginal effect on charge transport but effectively reduces the relaxation time for thermal transport.[21] Thus, the electrical EMFP is always higher than the thermal EMFP, and the difference becomes larger as temperature drops.

Fig. 2d displays the Lorenz number of the nanowire and bulk silver.[18,19] The resulting Lorenz number increases with temperature, displaying a similar trend as reported for silver,[5,6] platinum,[26] and gold[27] nanowires or thin films. At room temperature, the nanowire has a comparable Lorenz number with bulk silver. However, as temperature decreases, the Lorenz number of the nanowire becomes higher than the bulk value. Based on the Matthiessen's rule, the size effect on the EMFP of the nanowire can be written as $1/l_{e,nw} = 1/l_{e,bulk} + 1/l_b$, and $1/l_{th,nw} = 1/l_{th,bulk} + 1/l_b$, where $l_{e,bulk}$ and $l_{th,bulk}$ are the electrical and thermal EMFP of bulk silver, respectively; and l_b is the EMFP due to the electron-boundary scattering with the nanowire surface. When the lattice thermal conductivity is neglected in the 84 nm nanowire, the Lorenz number of the nanowire, $L_{nw} \propto \frac{l_{th,nw}}{l_{e,nw}} = \frac{l_{th,bulk}}{l_{e,bulk}} \times \frac{l_{e,bulk}+l_b}{l_{th,bulk}+l_b} \propto L_{bulk} \times \frac{l_{e,bulk}+l_b}{l_{th,bulk}+l_b}$. The ratio $\left(l_{e,bulk} + l_b\right)/\left(l_{th,bulk} + l_b\right)$ is larger than unity and gets larger as temperature drops, which leads to the higher nanowire Lorenz number at lower temperature.

The Lorenz number *versus* temperature for four silver nanowires of different sizes is plotted in Fig. 3a, which shows a clear size dependence with higher values for smaller wires. To further clarify the size dependence, we normalize the room-temperature thermal conductivity, electrical conductivity and Lorenz number for different size wires with respect to the corresponding values for the 84 nm wire, as shown in Fig. 3b. Both the thermal and electrical conductivities decrease for smaller wires as a result of enhanced boundary scattering; and the electrical conductivity decreases to a greater level, giving rise to an escalating Lorenz number. Fig. 3c and 3d plot the

thermal conductivity and electrical resistivity of four different size wires and the corresponding thermal and electrical conductivity reduction between the 84 nm and 38 nm wires, respectively. In the entire temperature range, the electrical conductivity reduces to a larger extent as compared to thermal conductivity, giving rise to a higher Lorenz number for smaller wires. First principles calculations have suggested that at 300 K electrons are with MFPs of 10-100 nm and phonons are with MFPs of 1-10 nm in silver.[25] Therefore, for nanowires with a diameter range of 38-84 nm, boundary scattering could significantly suppress the electron contribution to the thermal conductivity, while the size effect on phonon transport is still marginal. As such, the phonon contribution to the thermal conductivity becomes more significant for smaller wires. This renders the observed more significant reduction of electrical conductivity than thermal conductivity, and hence the enhanced Lorenz number for small diameter wires.

However, our analysis indicates that eliminating the phonon contributions by assuming that the lattice thermal conductivity remains to be 4.6 W/m-K for all nanowires, the Lorenz number based purely on electron transport, $L_e = \frac{\kappa_e}{\sigma T}$, still increases as the wire diameter decreases (Fig. S6). As mentioned previously, elastic stiffening occurs in silver nanowires of < 100 nm diameters with an increasing Young's modulus for smaller wires. However, the effects of elastic stiffening on transport properties of silver nanowires have not been examined.

To further dissect the effects of elastic stiffening on electrical and thermal transport in silver nanowires, we first model the electrical resistivity for the nanowires. From the measured Young's modulus (E) data for silver nanowires,[12] we performed a curve fitting (see Fig. S7) to extract the values for the four nanowires and derived their corresponding Θ_D. Then following the same procedure as we have done for the 84 nm diameter wire, we fit for the three smaller diameter wires. In the fitting, ρ_0 is fixed to be the same value as that for the 84 nm wire, which given the same

nanowire synthesis procedure, is a reasonable assumption. Importantly, the fitting is not sensitive to the value of ρ_0 as boundary scattering plays a much more important role at low temperature. Then we use p and $\alpha_{e\text{-}ph}$ as two fitting parameters to recapture the experimental data and the best values are listed in Table 1.

The resulting p value is between 0.65 and 0.47, indicating a significant portion of surface scattering is specular reflection. Note that the measured thermal conductivity in our work is about twice the predicted value based on the Boltzmann transport equation (BTE) with fully diffuse electron-boundary scattering,[28] which suggests that the obtained p is in a reasonable range. The specularity parameter p gets smaller progressively for smaller wires, which could be due to the stronger edge effect in the pentagonal cross-section. $\alpha_{e\text{-}ph}$ increases by almost 10% as the nanowire diameter decreases from 84 to 38 nm. One possible reason is that as suggested by a few publications, the e-ph coupling factor in nanostructures gets enhanced, which could lead to a larger $\alpha_{e\text{-}ph}$.[29–31] The overall e-ph scattering rate ($1/\tau_{e\text{-}ph}$, where $\tau_{e\text{-}ph}$ is the relaxation time) that is proportional to $\rho_{e\text{-}ph}$, however, reduces as the nanowire diameter decreases, owing to that the rest terms in Eq. (2) drops as Θ_D increases. This is also consistent with that the e-ph relaxation time is proportional to the square of the phonon group velocity,[21,32] which means that as the Young's modulus increases, the e-ph scattering rate reduces.

With reduced e-ph scattering rate, boundary scattering will play a more significant role in determining the EMFP; and if boundary scattering can effectively limit the electrical and thermal EMFP to the same value, the Lorenz number should be simply the Sommerfeld value. However, as Fig. 3a indicates, the Lorenz number for smaller nanowires can be actually higher than the Sommerfeld value, and the difference for the smallest wire is ~6.3% at room temperature, well beyond the phonon contribution of ~1.7% if we take κ_{ph} as the bulk value. This means that for

silver nanowires, κ_{ph} will be much higher than that of the bulk silver, which can be attributed to several changes induced by elastic stiffening. First, elastic stiffening corresponds to a higher speed of sound, which is directly proportional to κ_{ph}. In addition, the higher Θ_D shifts the phonon distribution to lower wave vectors at any given temperature, which should reduce the Umklapp scattering rate. Moreover, as discussed above, the e-ph scattering rate also becomes smaller. The overall effect is significantly enhanced lattice thermal conductivity that renders a Lorenz number higher than the Sommerfeld value for small nanowires. Actually if we take the room temperature Lorenz number purely due to electron transport as the Sommerfeld value, the lattice thermal conductivity for the 38 nm wire can be derived as 17.5 W/m-K, over three times that of the bulk value of 4.6 W/m-K.

It is worth noting that the elastic stiffening in penta-twinned Ag nanowires is likely originated from both the surface atom reconstruction and compression at the twin boundaries,[12,33] which leads to a rather uniform enhancement of Young's modulus across the wire cross-section. As such, we consider the elastic stiffening effects on transport properties based on an effective average value of the Young's modulus for the entire nanowire.

As contacts can play an critical role in the properties of composites, we seek to extract the electrical and thermal contact resistance between individual silver nanowires with D_h = 65 nm (Fig. 4a), following the same approach for multi-wall carbon nanotubes (MWCNTs).[34] The measured electrical and thermal resistance of the single (R_s) and contacted nanowires ($R_{t,contact}$) are plotted in Fig. 4c and 4d. The contact resistance (R_c) can be derived according to $R_c = R_{t,contact} - R_s/L_s \times L_c$,[34,35] which are about one-tenth of the measured total resistance of the single and contact samples. This relatively low weight of the contact resistance results in significantly fluctuated results even though the fluctuation in the measured total resistance is relatively small. Although the extracted R_c carries

quite a large uncertainty, useful information can still be derived. At 300 K, compared to the contact thermal resistance of ~1.8×10^7 K/W between two 63 nm diameter MWCNTs,[34] the contact thermal resistance between two 65 nm diameter silver wires is only 7.70×10^5 K/W, ~22 times lower, which suggests that silver nanowires could be much more effective nanofillers to enhance the thermal conductivity of nanocomposites.

To understand the much lower contact thermal resistance, we solve for the contact thermal conductance per unit area (G_{CA}). Fig. 4b shows an SEM micrograph of the wire-wire junction with a contact area of 107.0 ± 17.6 nm^2, which is ~2 times that between two MWCNTs of similar diameters. The significantly larger contact area could be due to the pentagonal cross-section of the silver wires. The calculated G_{CA} is 12.1×10^9 W/K-m^2, which falls in the range of 4-14×10^9 W/K-m^2 for some metal-metal interfaces,[36,37] but represents ~10 times that between MWCNTs. Possible reasons for this higher contact conductance are as follows. First, the thermal EMFP is ~ 37 nm at 300 K, much less than ~200 nm for phonons propagating along the radial direction in MWCNTs. This eliminates reflection of energy carriers back to the emitting tube/wire, which is one important factor for the low G_{CA} at MWCNT contacts.[34] Furthermore, it has been shown that Joule heating during electrical measurement could help to enhance the bonding between metal nanowires,[38,39] which could also facilitate transmission of energy carriers through the contact.

Fig. 4e shows the derived Lorenz number of the single wire and contact samples. While the relatively low weight of the contact in the total resistance renders the overall Lorenz numbers of the single and contact samples very close to each other, the extracted Lorenz number of the contact, even though with quite significant fluctuations, is clearly higher than the Sommerfeld value. The reason for this is that the extracted contact thermal conductance, 12.1×10^9 W/K-m^2, is still ~100 times smaller than the conductance of a pseudo-interface in bulk silver as estimated by κ_{bulk}/a,

where a is the lattice constant. As electrons are the dominant energy carriers in silver, this remarkable reduction indicates that the contact presents significant resistance to electron transport. On the other hand, the relative contribution of phonons in the contact thermal conductance could be more significant as phonons have a much smaller MFP than electrons. The combined effects lead to a larger Lorenz number at the contact.

In summary, systematic studies at the individual nanowire level provide direct experimental evidence of altered Lorenz numbers in silver nanowires. The clear trend of increasing Lorenz numbers for smaller wires comes mainly from the effects of elastic stiffening, which results in reduced e-ph scattering rates and higher Debye temperatures. These changes significantly enhance the phonon contribution to thermal transport, while the electron contribution is suppressed because boundary scattering effectively limits the electron MFP in silver nanowires. Importantly, the study provides experimental data on the contact thermal conductance per unit area, which is ~ 10 times that between MWCNTs, indicating one important factor that renders silver nanowires more effective nanofillers for enhancing the thermal conductivity of nanocomposites. This study discloses interesting transport mechanisms and provides important insights into designing silver nanowire-based composites.

Associated Content

Supporting Information

The Supporting Information is available free of charge on the ACS Publications website (https://pubs.acs.org).

Sample preparation, measurement method, cross-sectional area characterization and experimental uncertainty; effects of wire-membrane contact thermal resistance and wire bending; electrical

resistivity fitting with Bloch-Grüneisen formula; effects of phonons on the Lorentz number; Young's modulus derivation (PDF).

Author Contributions

Y.Z. and M.F. conducted measurements. Y.Z. and Y.T. performed theoretical analyses. Y.Z. and D.L. prepared the manuscript. D.L. and G.S. supervised the project. D.L., G.S., D.X., and Y.Z. edited the manuscript. All authors discussed the results and commented on the manuscript.

Notes

The authors declare no competing financial interest.

Acknowledgements

The authors thank the financial support from the U.S. National Science foundation (Award#1903645 and #1532107). Matthew L. Fitzgerald acknowledges the graduate fellowship support from the National Aeronautics and Space Administration (NSTRF18_80NSSC18K1165). The work was performed in part at Cornell Nanoscale Facility, an NNCI member supported by NSF Grant NNCI-1542081.

Reference

(1) Hsu, P.-C.; Liu, X.; Liu, C.; Xie, X.; Lee, H. R.; Welch, A. J.; Zhao, T.; Cui, Y. Personal Thermal Management by Metallic Nanowire-Coated Textile. *Nano Letters* **2015**, *15*, 365–371.

(2) Yu, Z.; Li, L.; Zhang, Q.; Hu, W.; Pei, Q. Silver Nanowire-Polymer Composite Electrodes for Efficient Polymer Solar Cells. *Advanced Materials* **2011**, *23*, 4453–4457.

(3) Kang, S.; Kim, T.; Cho, S.; Lee, Y.; Choe, A.; Walker, B.; Ko, S.-J.; Kim, J. Y.; Ko, H. Capillary Printing of Highly Aligned Silver Nanowire Transparent Electrodes for High-Performance Optoelectronic Devices. *Nano Letters* **2015**, *15*, 7933–7942.

(4) Cho, S.; Kang, S.; Pandya, A.; Shanker, R.; Khan, Z.; Lee, Y.; Park, J.; Craig, S. L.; Ko, H. Large-Area Cross-Aligned Silver Nanowire Electrodes for Flexible, Transparent, and Force-Sensitive Mechanochromic Touch Screens. *ACS Nano* **2017**, *11*, 4346–4357.

(5) Kojda, D.; Mitdank, R.; Handwerg, M.; Mogilatenko, A.; Albrecht, M.; Wang, Z.; Ruhhammer, J.; Kroener, M.; Woias, P.; Fischer, S. F. Temperature-Dependent Thermoelectric Properties of Individual Silver Nanowires. *Physical Review B* **2015**, *91*, 24302.

(6) Cheng, Z.; Liu, L.; Xu, S.; Lu, M.; Wang, X. Temperature Dependence of Electrical and Thermal Conduction in Single Silver Nanowire. *Scientific Reports* **2015**, *5*, 10718.

(7) He, G.-C.; Lu, H.; Dong, X.-Z.; Zhang, Y.-L.; Liu, J.; Xie, C.-Q.; Zhao, Z.-S. Electrical and Thermal Properties of Silver Nanowire Fabricated on a Flexible Substrate by Two-Beam Laser Direct Writing for Designing a Thermometer. *RSC Advances* **2018**, *8*, 24893–24899.

(8) He, G.-C.; Dong, X.-Z.; Liu, J.; Lu, H.; Zhao, Z.-S. Investigate the Electrical and Thermal Properties of the Low Temperature Resistant Silver Nanowire Fabricated by Two-Beam Laser Technique. *Applied Surface Science* **2018**, *439*, 96–100.

(9) Wang, J.; Wu, Z.; Mao, C.; Zhao, Y.; Yang, J.; Chen, Y. Effect of Electrical Contact Resistance on Measurement of Thermal Conductivity and Wiedemann-Franz Law for Individual Metallic Nanowires. *Scientific Reports* **2018**, *8*, 4862.

(10) Jing, G. Y.; Duan, H. L.; Sun, X. M.; Zhang, Z. S.; Xu, J.; Li, Y. D.; Wang, J. X.; Yu, D. P. Surface Effects on Elastic Properties of Silver Nanowires: Contact Atomic-Force Microscopy. *Physical Review B* **2006**, *73*, 235409.

(11) Cuenot, S.; Frétigny, C.; Demoustier-Champagne, S.; Nysten, B. Surface Tension Effect on the Mechanical Properties of Nanomaterials Measured by Atomic Force Microscopy. *Physical Review B* **2004**, *69*, 165410.

(12) Chang, T.-H.; Cheng, G.; Li, C.; Zhu, Y. On the Size-Dependent Elasticity of Penta-Twinned Silver Nanowires. *Extreme Mechanics Letters* **2016**, *8*, 177–183.

(13) Wingert, M. C.; Kwon, S.; Hu, M.; Poulikakos, D.; Xiang, J.; Chen, R. Sub-Amorphous Thermal Conductivity in Ultrathin Crystalline Silicon Nanotubes. *Nano Letters* **2015**, *15*, 2605–2611.

(14) Yang, L.; Yang, Y.; Zhang, Q.; Zhang, Y.; Jiang, Y.; Guan, Z.; Gerboth, M.; Yang, J.; Chen, Y.; Greg Walker, D.; *et al.* Thermal Conductivity of Individual Silicon Nanoribbons. *Nanoscale* **2016**, *8*, 17895–17901.

(15) Yang, L.; Tao, Y.; Liu, J.; Liu, C.; Zhang, Q.; Akter, M.; Zhao, Y.; Xu, T. T.; Xu, Y.; Mao, Z.; *et al.* Distinct Signatures of Electron–Phonon Coupling Observed in the Lattice Thermal Conductivity of NbSe3 Nanowires. *Nano Letters* **2019**, *19*, 415–421.

(16) Zhang, Q.; Liu, C.; Liu, X.; Liu, J.; Cui, Z.; Zhang, Y.; Yang, L.; Zhao, Y.; Xu, T. T.; Chen, Y.; *et al.* Thermal Transport in Quasi-1D van Der Waals Crystal Ta2Pd3Se8 Nanowires: Size and Length Dependence. *ACS Nano* **2018**, *12*, 2634–2642.
(17) Hochbaum, A. I.; Chen, R.; Delgado, R. D.; Liang, W.; Garnett, E. C.; Najarian, M.; Majumdar, A.; Yang, P. Enhanced Thermoelectric Performance of Rough Silicon Nanowires. *Nature* **2008**, *451*, 163–167.
(18) Ho, C. Y.; Powell, R. W.; Liley, P. E. Thermal Conductivity of the Elements: A Comprehensive Review. *Journal of Physical and Chemical Reference Data* **1974**, *3*, 1–796.
(19) Matula, R. A. Electrical Resistivity of Copper, Gold, Palladium, and Silver. *Journal of Physical and Chemical Reference Data* **1979**, *8*, 1147–1298.
(20) *Thermal Conductivity*; Tritt, T. M., Ed.; Physics of Solids and Liquids; Springer US: New york, 2004.
(21) Ziman, J. M. *Electrons and Phonons: The Theory of Transport Phenomena in Solid*; Oxford University Press, 2001.
(22) R. G. Chambers. The Conductivity of Thin Wires in a Magnetic Field. *Proceedings of the Royal Society of London. Series A. Mathematical and Physical Sciences* **1950**, *202*, 378–394.
(23) Steinhögl, W.; Schindler, G.; Steinlesberger, G.; Engelhardt, M. Size-Dependent Resistivity of Metallic Wires in the Mesoscopic Range. *Physical Review B* **2002**, *66*, 75414.
(24) Kittel, C. *Introduction to Solid State Physics*; 8th editio.; Wiley, New York, 2004.
(25) Jain, A.; McGaughey, A. J. H. Thermal Transport by Phonons and Electrons in Aluminum, Silver, and Gold from First Principles. *Physical Review B* **2016**, *93*, 81206.
(26) Völklein, F.; Reith, H.; Cornelius, T. W.; Rauber, M.; Neumann, R. The Experimental Investigation of Thermal Conductivity and the Wiedemann–Franz Law for Single Metallic Nanowires. *Nanotechnology* **2009**, *20*, 325706.
(27) Sawtelle, S. D.; Reed, M. A. Temperature-Dependent Thermal Conductivity and Suppressed Lorenz Number in Ultrathin Gold Nanowires. *Physical Review B* **2019**, *99*, 54304.
(28) Stojanovic, N.; Maithripala, D. H. S.; Berg, J. M.; Holtz, M. Thermal Conductivity in Metallic Nanostructures at High Temperature: Electrons, Phonons, and the Wiedemann-Franz Law. *Physical Review B* **2010**, *82*, 75418.
(29) Qiu, T. Q.; Tien, C. L. Size Effects on Nonequilibrium Laser Heating of Metal Films. *Journal of Heat Transfer* **1993**, *115*, 842–847.
(30) Timalsina, Y. P.; Horning, A.; Spivey, R. F.; Lewis, K. M.; Kuan, T.-S.; Wang, G.-C.; Lu, T.-M. Effects of Nanoscale Surface Roughness on the Resistivity of Ultrathin Epitaxial Copper Films. *Nanotechnology* **2015**, *26*, 75704.
(31) Timalsina, Y. P.; Shen, X.; Boruchowitz, G.; Fu, Z.; Qian, G.; Yamaguchi, M.; Wang, G.-C.; Lewis, K. M.; Lu, T.-M. Evidence of Enhanced Electron-Phonon Coupling in Ultrathin Epitaxial Copper Films. *Applied Physics Letters* **2013**, *103*, 191602.
(32) Asheghi, M.; Kurabayashi, K.; Kasnavi, R.; Goodson, K. E. Thermal Conduction in Doped Single-Crystal Silicon Films. *Journal of Applied Physics* **2002**, *91*, 5079–5088.
(33) Niekiel, F.; Spiecker, E.; Bitzek, E. Influence of Anisotropic Elasticity on the Mechanical Properties of Fivefold Twinned Nanowires. *Journal of the Mechanics and Physics of Solids* **2015**, *84*, 358–379.
(34) Yang, J.; Shen, M.; Yang, Y.; Evans, W. J.; Wei, Z.; Chen, W.; Zinn, A. A.; Chen, Y.;

Prasher, R.; Xu, T. T.; *et al.* Phonon Transport through Point Contacts between Graphitic Nanomaterials. *Physical Review Letters* **2014**, *112*, 205901.
(35) Yang, J.; Waltermire, S.; Chen, Y.; Zinn, A. A.; Xu, T. T.; Li, D. Contact Thermal Resistance between Individual Multiwall Carbon Nanotubes. *Applied Physics Letters* **2010**, *96*, 23109.
(36) Gundrum, B. C.; Cahill, D. G.; Averback, R. S. Thermal Conductance of Metal-Metal Interfaces. *Physical Review B* **2005**, *72*, 245426.
(37) Wilson, R. B.; Cahill, D. G. Experimental Validation of the Interfacial Form of the Wiedemann-Franz Law. *Physical Review Letters* **2012**, *108*, 255901.
(38) Vafaei, A.; Hu, A.; Goldthorpe, I. A. Joining of Individual Silver Nanowires via Electrical Current. *Nano-Micro Letters* **2014**, *6*, 293–300.
(39) Song, T.-B.; Chen, Y.; Chung, C.-H.; Yang, Y. (Michael); Bob, B.; Duan, H.-S.; Li, G.; Tu, K.-N.; Huang, Y.; Yang, Y. Nanoscale Joule Heating and Electromigration Enhanced Ripening of Silver Nanowire Contacts. *ACS Nano* **2014**, *8*, 2804–2811.

Figures

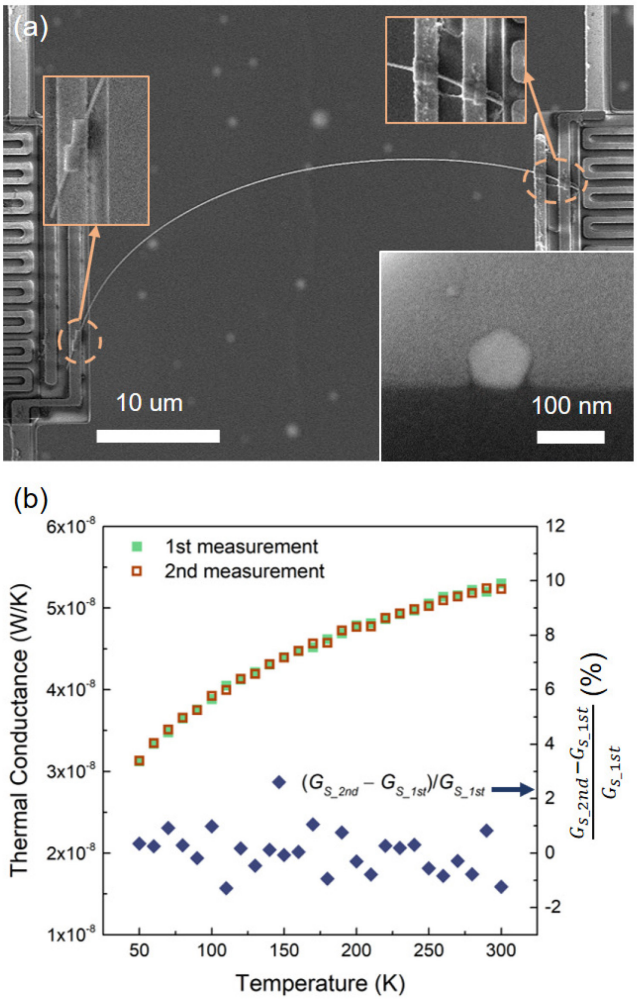

Figure 1. Effects of contact thermal resistance. (a) The SEM micrograph of a silver nanowire placed on a 36 μm-gap device with two rounds of Pt/C deposition at the wire-suspended membrane contacts. The inset shows the cross-section of the wire with D_h = 89 nm. (b) The measured thermal conductance after the first and second round of EBID essentially overlaps (with < 2% difference).

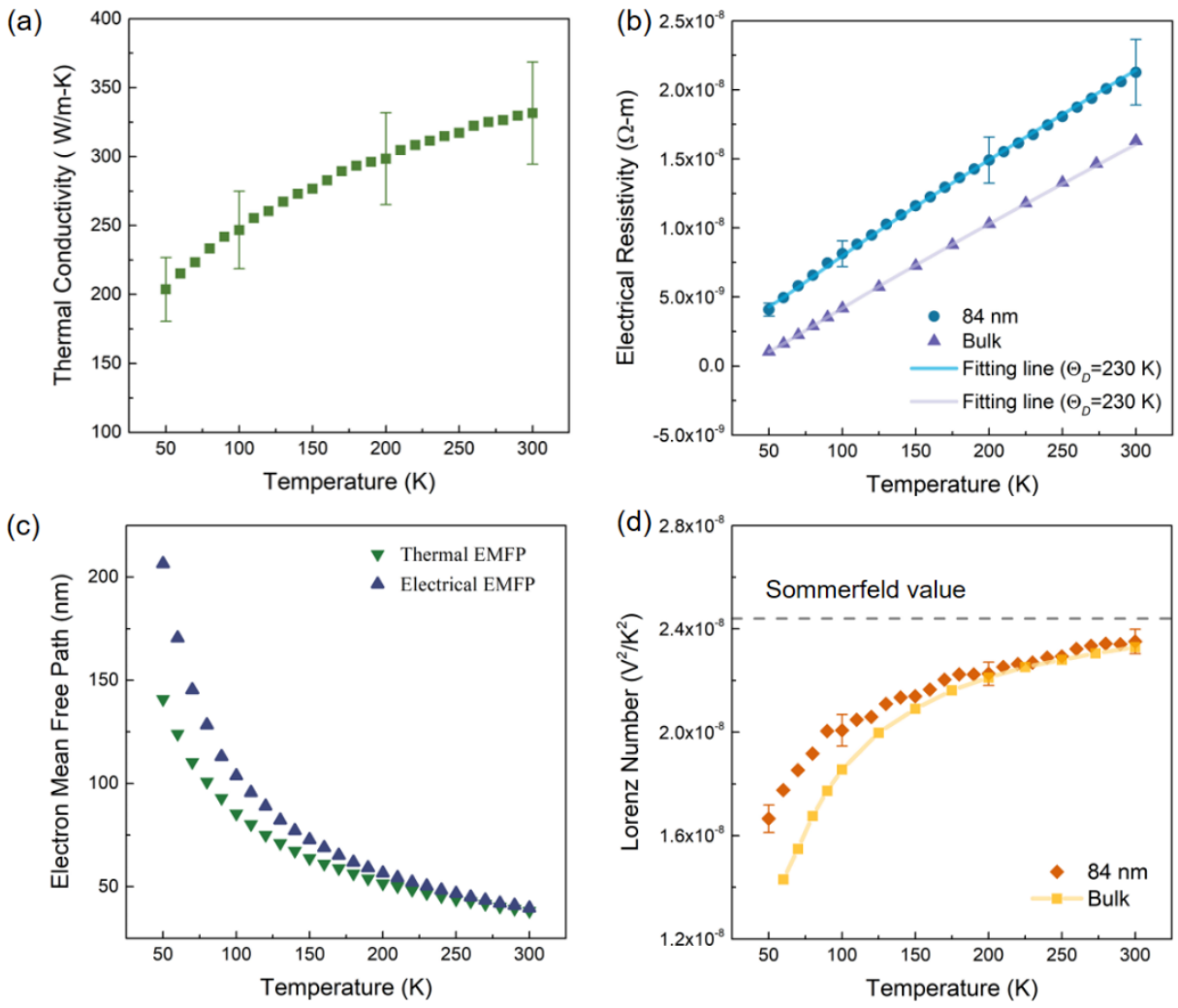

Figure 2. Thermal and electrical properties of an individual silver nanowire with D_h = 84 nm and L_s = 44 μm. (a) Temperature dependence of thermal conductivity. (b) Electrical resistivity of the nanowire and bulk silver[19]. The bulk resistivity is fitted with Eq. (2)-(3) and the fitting line for the nanowire is achieved from Eq. (2)-(5). (c) Thermal and electrical EMFP derived from the measured thermal and electrical conductivity. (d) Lorenz number of the nanowire and bulk silver. The bulk value is calculated with the experimental thermal conductivity[18] and electrical resistivity[19].

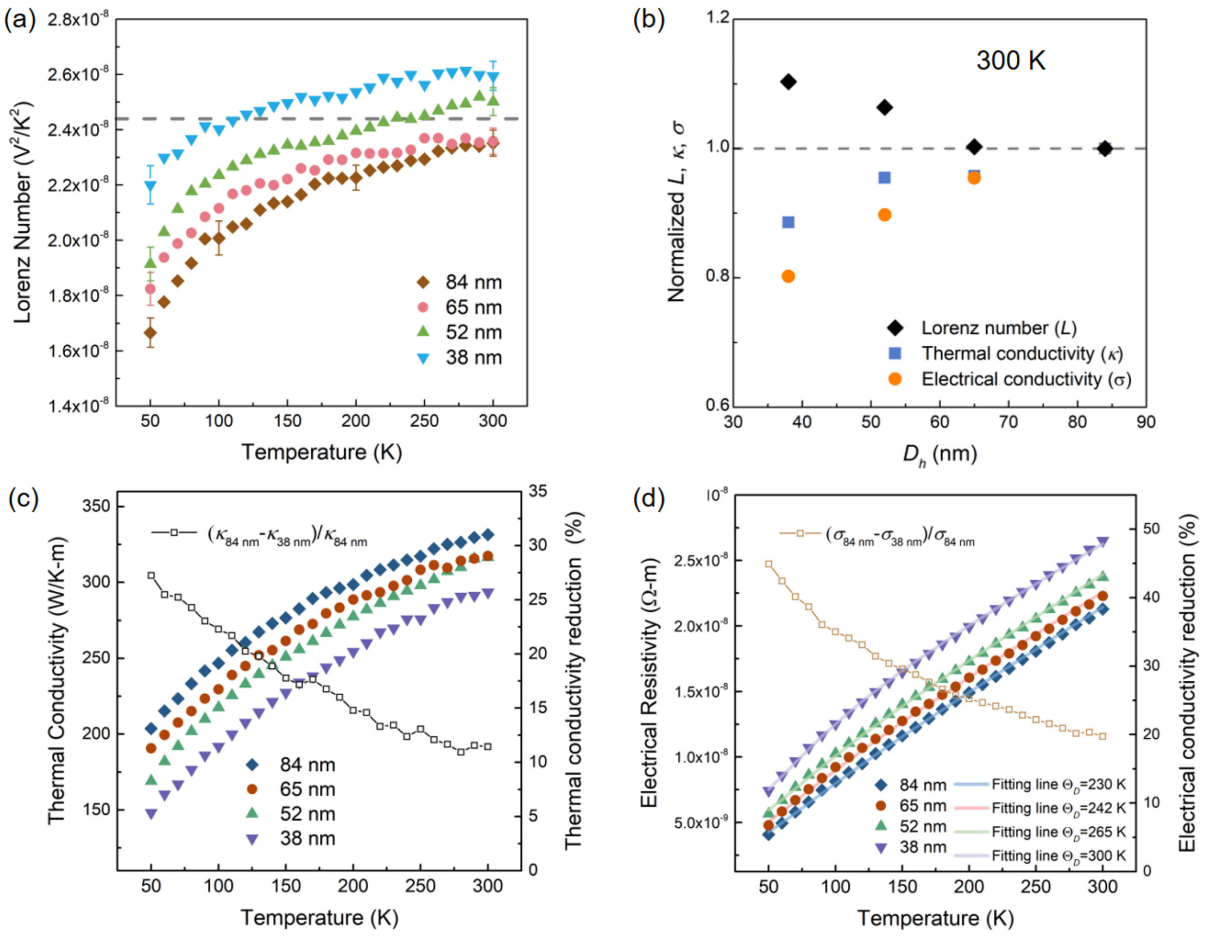

Figure 3. Size dependence of transport properties. (a) Derived Lorenz number of four different diameter silver nanowires. The grey dash line labels the Sommerfeld number. (b) Normalized thermal conductivity, electrical conductivity and Lorenz number with respect to the respective values of the 84 nm diameter nanowire at 300 K. The grey dash line separates the enhanced Lorenz number and reduced thermal and electrical conductivity as size decreases. (c) Thermal conductivity of the four nanowires and the thermal conductivity reduction between the 84 nm and 38 nm wires. (d) Electrical resistivity of the four nanowires and electrical conductivity reduction between the 84 nm and 38 nm wires. The Debye temperature used for the fitting lines is 230 K, 242 K, 265 K and 300 K, respectively. The uncertainty for the thermal conductivity and electrical resistivity is ~12% and ~11%, respectively.

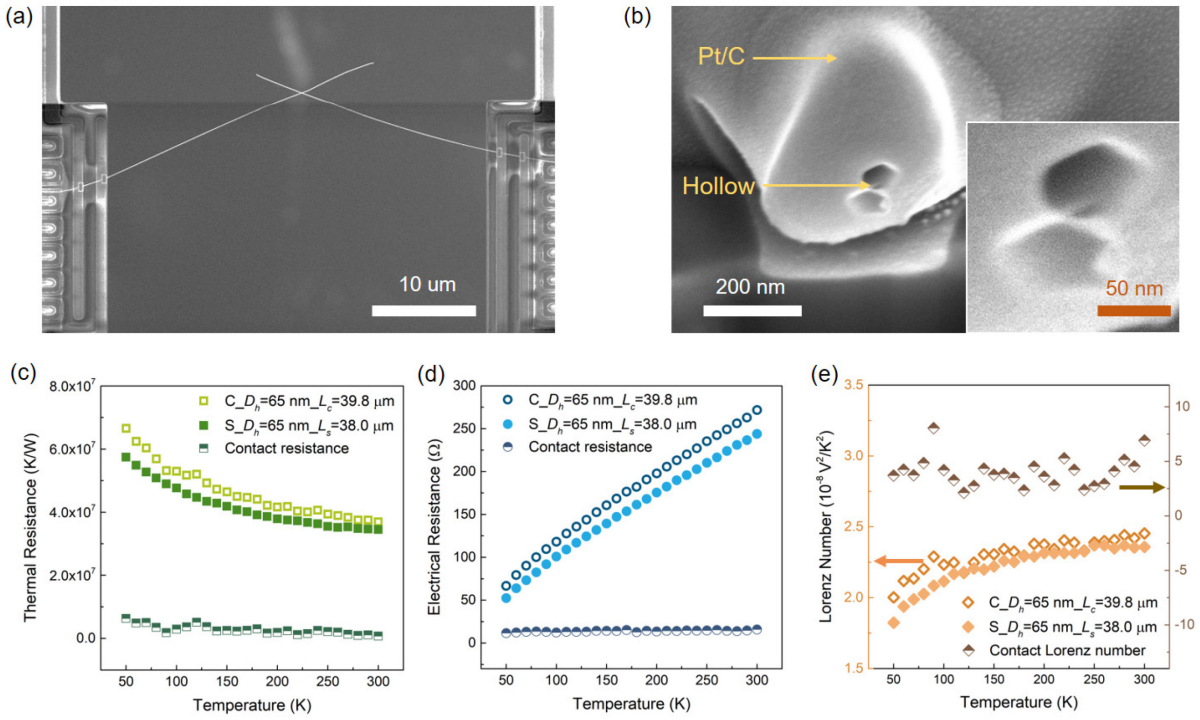

Figure 4. Thermal and electrical properties at an individual contact between two silver nanowires. (a) SEM image of two contacted silver nanowires with D_h = 65 nm and L_c = 39.8 μm. (b) SEM image of cross-sectional cutting of contacted silver nanowires tilted at 52°. The inset is the zoom-in image of the contact configuration. (c) Thermal and (d) Electrical resistance of single and contacted nanowires as well as their contact resistance. (e) Lorenz number of single and contacted nanowires and their contact Lorenz number *versus* temperature. The arrow guides the vertical coordinate used for the three sets of data. The capital S and C in legends denote the single and contacted silver nanowires, respectively. We note that the lengths of the contact sample and the single wire sample are slightly different by 4.7%. The contact resistance between the two wires (R_c) is derived according to $R_c = R_{t,contact} - R_s/L_s \times L_c$.

Table 1. The parameters used for the fitting lines for the bulk silver and nanowires.

D_h (nm)	Normalized E	Θ_D (K)	ρ_0 (10^{-11} Ω-m)	$\alpha_{e\text{-}ph}$ (10^{-8} Ω-m)	p
bulk	1	230	1.0	5.08	
84	1	230	8.15	5.782	0.65
65	1.11	242	8.15	5.996	0.62
52	1.33	265	8.15	6.149	0.60
38	1.71	300	8.15	6.314	0.47

Table of Content